Available online at www.sciencedirect.com
SCIENCE DIRECT®
Applied Numerical Mathematics 51 (2004) 463–475
APPLIED NUMERICAL MATHEMATICS
www.elsevier.com/locate/apnum

A partition method for the solution of a coupled liquid-structure interaction problem

Edoardo Bucchignani [a,*], Fulvio Stella [b], Fabio Paglia [b]

[a] *Centro Italiano Ricerche Aerospaziali, Via Maiorise, 81043 Capua, CE, Italy*
[b] *Dipartimento di Meccanica e Aeronautica, Via Eudossiana 18, 00184 Roma, Italy*

Available online 12 August 2004

Abstract

A numerical code is presented to study the motion of an incompressible inviscid flow in a deformable tank. It is based on a method belonging to the partition treatment class, as the fluid and structural fields are solved by coupling two distinct models. The fluid field is modeled by the Laplace equation and numerically solved by a Finite Volume technique. The computational grid is updated at each time step to take into account the movements of the free surface and the deformations of the vertical walls. An unsteady finite element formulation is used for modeling the tank on a grid discretized by triangular elements and linear shape functions. Results are presented for two different cases: a flow induced by a perturbation on the free surface in a tank motionless; a flow in a tank forced to oscillate periodically in the horizontal direction.

Keywords: Fluid-structure interaction; Sloshing; Aerospace

1. Introduction

The coupling of unsteady fluid flow and structure motion is an important field of computational mechanics [1,2]. The behavior of the fluid flow and the structure are dependent on each other. The development of numerical methods to solve these problems is a challenging issue. Accurate computation of unsteady flow and concurrent updating of the fluid grid are required to calculate the fluid-structure interaction. This issue is very interesting in the field of aerospace, even for possible applications to the launchers of the next generations. In fact the problem of tank security is particularly felt, because spatial

* Corresponding author.
E-mail addresses: e.bucchignani@cira.it (E. Bucchignani), fulvio@stella.ing.uniroma1.it (F. Stella), fabio@stella.ing.uniroma1.it (F. Paglia).

0168-9274/$30.00 © 2004 IMACS. Published by Elsevier B.V. All rights reserved.
doi:10.1016/j.apnum.2004.06.004

vehicles carry large quantities of fluids; when a tank is subjected to periodic forces, large amplitude vibrations are induced along the walls. Besides, the fluid movement of the free surface, named as *sloshing*, may induce a resonance condition if the oscillations are at a determinate frequency. A partially filled tank will experience violent fluid motion when subjected to periodic forces containing energy in the vicinity of the natural periods for the fluid motion inside the tank. Since *sloshing* is a typical resonance phenomenon, it is not necessarily the most extreme external force that causes the most severe conditions. As a consequence, the study of the *sloshing* is important in order to determine the structural requirement of the tank. It is simple to observe that the fluid domain contours move under the action of the liquid pressure, causing a variation of the fluid dynamics boundary conditions; therefore the study of the flow field and the structural behavior cannot be treated separately, otherwise considerable errors could be noticed.

The methodologies used for the solutions of fluid-structure interaction problems can be subdivided into the following groups: field elimination [3], partition treatment [4] and simultaneous treatment [5]. In the first case, the structural calculus is decoupled from the fluid dynamics one by means of simple integral transformations. The use of these methodologies is recommended only for linear problems with few degrees of freedom. In the second case, the fluid and structural fields are solved using two distinct models that are mathematically formulated on two different computational domains. These computational domains are suitably interfaced for data exchanging. In the last case, an implicit coupling is performed between fluid and structure. The governing equations are written independently using the most suitable formulation for each field (e.g., finite volume for the fluid, finite element for the structure) and solving simultaneously all the algebraic equations obtained.

In this paper we present a numerical code capable of simulating the motion of an incompressible fluid in a two-dimensional domain bounded by elastic-deformable walls, with an open top surface mobile and free. A partition treatment has been adopted, and two distinct mathematical models have been used respectively for the fluid (CFD) and for the structure (CSD). Discretization of the governing equation for the flow is conducted via a second-order finite volume technique on a grid with quadrilateral elements. The grid is updated at each time step, keeping into account the movements of the free surface and the deformations of the solid walls. The pressure distribution along the walls is interpolated using a second-order polynomial approximation. The governing equations for the structure have been discretized with an unsteady finite element formulation, using triangular elements with linear shape functions. As the two computational grids are connected without continuity, the data exchange between the two solvers is not immediate, but requires some interpolation operations. The data transfer from CFD to CSD is realized by evaluating the forces acting on the nodes of the solid interface starting from the values of the pressure in the nodes of the liquid interface. The data transfer from CSD to CFD is performed by a simple data interpolation on the deformations. The fluid dynamics approach is proven to be efficient from a computational point of view and flexible, as it allows to solve a large variety of problems, both at earthly gravity and in microgravity conditions. A great accuracy in the time histories and mass conservation is achieved [6]. The CSD solver is a traditional one, but it provides accurate results: in fact, the structural deformation phenomenon is much more regular if compared with the fluid motion and therefore particular care is not required.

In this paper a square tank whose walls are made up of steel is considered. The tank is filled with water and the gravity acceleration is equal to the earthly value. Two different cases have been considered: a flow induced by a perturbation on the free surface in a tank motionless; a flow in a tank forced to oscillate periodically in the horizontal direction (forced sway oscillations).

2. Mathematical model for the fluid dynamics

2.1. Formulation

The evolutions of waves on the surface of a fluid enclosed in a box is described by the equations governing the motion of the flow and appropriate boundary conditions (CFD). As we consider containers whose size is larger than the characteristic wavelengths, the surface tension and the viscous effects are neglected, while non-linear free surface effects are taken into account. We consider the case of an irrotational incompressible flow in a rectangular two dimensional box (width L, height H) with an open top free surface. We also assume that the amplitude of the oscillations is small if compared to the wavelength of the perturbation and to the depth of the box. All the physical quantities are referred to a coordinate system fixed with respect to the undeformed tank; so, in the case of a moving tank (forced sway oscillations), the apparent forces must be taken into account. The fluid motion is governed by the Laplace equation [7]:

$$\nabla^2\phi = \frac{\partial^2\phi}{\partial x^2} + \frac{\partial^2\phi}{\partial z^2} = 0, \tag{1}$$

where ϕ is the potential velocity and the components of the velocity vector $\mathbf{u}(u, w)$ are given by:

$$u = \frac{\partial\phi}{\partial x}, \qquad w = \frac{\partial\phi}{\partial z}.$$

As illustrated by Fig. 1, we assume that the waves propagate along x on the free surface. Let $\eta(x, t)$ be the function describing the wave height measured with respect to the undisturbed configuration. The boundary conditions are imposed in the following way.

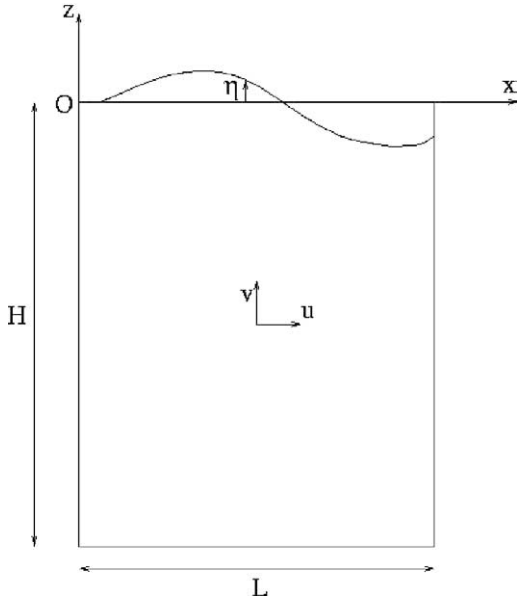

Fig. 1. Reference system for the fluid.

- On the solid walls of the box the compatibility condition on the velocity field is:

$$\mathbf{u} \cdot \mathbf{n} = \mathbf{u_s} \cdot \mathbf{n}, \tag{2}$$

  where $\mathbf{n}$ is the outward normal to the boundary and $\mathbf{u_s}$ is the velocity deformation of the wall.
- On the free surface, a cinematic and a dynamic conditions are imposed. The first one states that the velocity of the surface must be equal to the vertical component of velocity:

$$\frac{\partial \eta}{\partial t} + \frac{\partial \phi}{\partial x}\frac{\partial \eta}{\partial x} - \frac{\partial \phi}{\partial z}_{(z=\eta)} = 0. \tag{3}$$

The dynamic condition states that the pressure on the free surface is equal to the external one. The Bernoulli theorem can be successfully used; if the volume forces are reduced to the weight and the external pressure is set equal to zero, we obtain [8]:

$$\frac{\partial \phi}{\partial t} + \frac{1}{2}\left[\left(\frac{\partial \phi}{\partial x}\right)^2 + \left(\frac{\partial \phi}{\partial z}\right)^2\right] + g\eta + \frac{\partial \phi_c}{\partial t} = 0, \tag{4}$$

where g is the gravitational acceleration, $\partial \phi_c / \partial t$ is the acceleration of the tank with respect to an inertial coordinate system. Note that this last term vanishes if the tank is motionless. Finally, ϕ_c is related to the relative velocity of the tank by the relation:

$$\phi_c = \int u_t \, \mathrm{d}x.$$

This set of equations must be completed by suitable initial conditions to get a unique solution.

The Laplace equation (1) and the boundary conditions (2)–(4) have been set in non-dimensional form assuming the width of the tank L as reference length and the quantity $(L/g_0)^{1/2}$ as reference time (g_0 is the gravity acceleration at earthly level). The formulation presented here is independent of the tank support condition. At the end of each time step, the liquid pressure on the solid walls is evaluated using the Bernoulli equation [6]:

$$p = -\frac{\partial \phi}{\partial t} - \frac{1}{2}\left[\left(\frac{\partial \phi}{\partial x}\right)^2 + \left(\frac{\partial \phi}{\partial z}\right)^2\right] - gz - \frac{\partial \phi_c}{\partial t}$$

(the reference pressure for the a-dimensionalization is given by $\rho L g_0$).

2.2. Numerical implementation

A time-dependent algorithm has been used in order to obtain accurate true transient solutions. A Fully Implicit approach has been adopted for the time integration in order to guarantee high stability to the method. As shown in [9], this kind of approach represents a useful compromise among numerical efficiency, robustness and flexibility in applications. Particular care has been adopted for the treatment of the non-linear conditions on the free surface. The cinematic and dynamic conditions on the free surface have been linearized by means of the following approximations:

$$\frac{\partial \eta}{\partial t} + \frac{\partial \phi^*}{\partial x}\frac{\partial \eta}{\partial x} - \frac{1}{2}\left(\frac{\partial \phi^*}{\partial z} + \frac{\partial \phi}{\partial z}\right) = 0,$$

$$\frac{\partial \phi}{\partial t} + \frac{1}{2}\frac{\partial \phi^*}{\partial x}\frac{\partial \phi}{\partial x} + \frac{1}{2}\frac{\partial \phi^*}{\partial z}\frac{\partial \phi}{\partial z} + \frac{1}{2}g\left(\eta + \eta^*\right) = -\frac{\partial \phi_c}{\partial t},$$

where all the quantities are considered at the current time step, with the exception of the quantities marked with a $*$ that are considered at the previous time step. Few remarks can be made on this use of quantities evaluated at the previous time step. For what concerns the terms $\partial\phi/\partial z$ and η respectively in the first and second equation, the discrete form is obtained following the well-known Cranck–Nicholson formula [10,11]. Concerning the quadratic terms, since they are all non-linear, a linearization is required in order to approach the resulting algebraic problem with a linear solver. In this case one of the factors has been frozen at the previous time step, reducing the problem to a linear one [12]. This technique guarantees a good coupling between all the equations. As a result of the simplifying assumptions, the lack of viscosity may cause an undesirable contribution from the high frequency components to the numerical solution of the problem. This contribution is undesirable because the high frequency modes are poorly represented in the discretized system. As a consequence, a dispersion error may develop in the numerical solution. This effect may occur when the liquid is in the resonance zone or when the excitation level is relatively high. Numerical dissipation could be used to damp out the high frequency wave components propagating near the free surface, as proposed in [13]. However this strategy has not been considered in the present work, as our goal is the investigation of the system for small amplitude oscillations.

The Laplace equation has been discretized using a finite volume technique on a grid made up of quadrilateral elements.The computational grid is updated at each time step, in order to take into account the variation of the domain shape due to the movement of the free surface and of the solid walls. A transient procedure requires particular care, as the mass conservation could be violated. The staggering of the variable location provides the maximum accuracy of the discretized derivatives and ensures the discrete conservation of mass at each time step. In fact, as shown in reference [14], it is possible to obtain mass conservation to round off error if the horizontal velocity is located at the middle of the vertical face of the computational cell and the vertical velocity is located at the middle of the horizontal face. As a consequence, the potential ϕ is naturally located at the center of the cell. For what concerns the boundary conditions, spatial derivatives are discretized using two-point backward differences, while time derivatives are discretized using three-point backward differences. At each time step the original system of partial differential equations gives rise to a large linear system of equations of the type $\mathbf{A}x = b$, where x is the unknown vector. The coefficient matrix $\mathbf{A}$ has a large sparse structure. The solution of this linear system via a direct method is not recommended due to the size of the problem, so an iterative procedure has been preferred: the Bi-CGSTAB algorithm [15], associated with a ILU decomposition of the matrix $\mathbf{A}$ as preconditioner has been employed. The Bi-CGSTAB algorithm is an iterative method belonging to the class of the Krylov subspace methods; it has been chosen for its good numerical stability and speed of convergence even in dealing with non-symmetric problems, as shown in Refs. [16,9].

3. Mathematical model for the structure

When the walls of a tank are thin, their vibrations under the effects of variable liquid pressure cannot be neglected. In this case it is essential to develop a mathematical model (CSD) that keeps into account the deformations of the walls. It is assumed that the tank is made up of an elastic isotropic material and that the constitutive law is the Hook's one. The governing equations for the structure are the usual undefined equilibrium relations for continuous media. Under these hypothesis, a finite element discretization of the tank can be performed. If the displacement of the structure changes in the time, it is necessary to keep into account the inertial forces and the frictional resistances opposing the motion. These may be due to

microstructure movements, air resistance etc. As a consequence, the equilibrium general condition for the structure in a Finite Element formulation assumes the following expression [3]:

$$M\ddot{\mathbf{a}} + C\dot{\mathbf{a}} + K\mathbf{a} = \mathbf{f},$$

where **a** is the displacement vector, M, C and K are respectively the mass matrix, the damping matrix and the stiffness matrix; **f** is the force vector. All the matrices are obtained by assembling the matrices related to each element (M^e, C^e and K^e). K^e is obtained in accord with Ref. [17] as:

$$K^e = \int_s B^{\mathrm{T}} D B \, \mathrm{d}s,$$

where B is the strain-displacement matrix and D is the material matrix (depending on the Young modulus E and on the Poisson coefficient ν of the material). M^e is given by:

$$M^e = \int_s N^{\mathrm{T}} \rho N \, \mathrm{d}s,$$

where ρ is the density and N is the shape function matrix. The definition of C^e is in practice difficult and therefore it is assumed that C^e is a linear combination of stiffness and mass matrices; that is:

$$C^e = \alpha M^e + \beta K^e,$$

where α and β are determined experimentally.

The spatial discretization of the structure has been performed using triangular elements with linear shape functions (Fig. 2). The discretization of the time derivatives has been performed using Finite Difference approximations with a three-point formula for the second-order derivative and a two-point formula for the first-order derivative. Also in this case, the large sparse linear systems arising from discretization at each time step are solved using the Bi-CGSTAB algorithm without preconditioning.

4. Coupling between fluid and structural fields

The methodology used here for the solution of the fluid-structure interaction problems belongs to the partition treatment class. As described above, in a general approach the CFD and CSD solvers use different formulations and discretizations. The two computational grids are not continuously interconnected, in the sense that the nodes on the interface of the fluid domain do not coincide with the ones of the interface of the solid domain (Fig. 3). Therefore, the data exchange between the two solvers is not immediate, but requires some interpolation operations. The data transfer from CFD to CSD is realized by evaluating the forces acting on the nodes of the solid interface starting from the values of the pressure in the nodes of the liquid interface. This operation must be performed carefully, in such a way that the global energy of the system is conserved. The forces acting on the CSD nodes are [18]:

$$F_i = \int_s -N_i p_i n \, \mathrm{d}s,$$

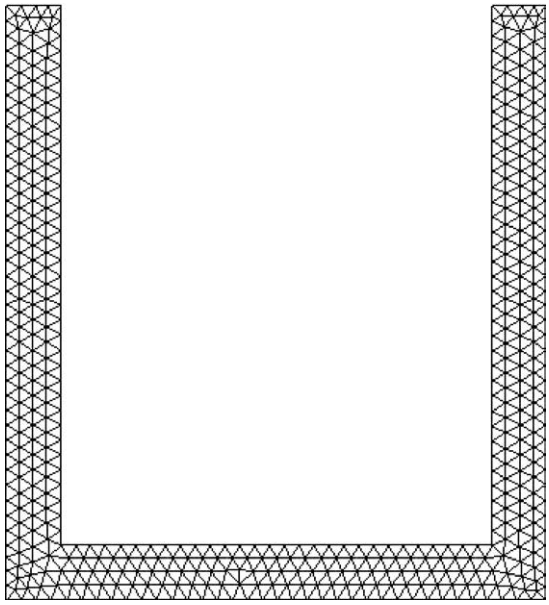

Fig. 2. An example of structural computational grid.

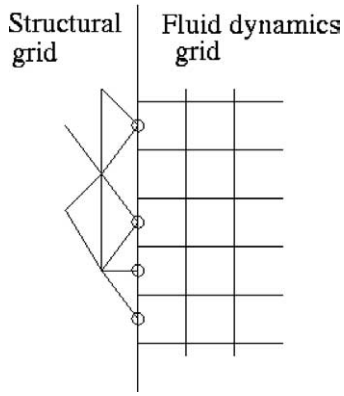

Fig. 3. Solid-fluid interface.

where the pressure p_i in the CSD nodes is the integral of the liquid pressure on the faces of the CSD cells (Fig. 4) [19]:

$$p_i = \frac{1}{\Delta x} \int_{x_i - \Delta x/2}^{x_i + \Delta x/2} p(x)\,\mathrm{d}x.$$

Otherwise, in many practical problems the liquid pressure distribution is rather regular and so it is convenient to have an analytical representation of the pressure distribution by means of a polynomial interpolation; in this case a second-order polynomial is adopted.

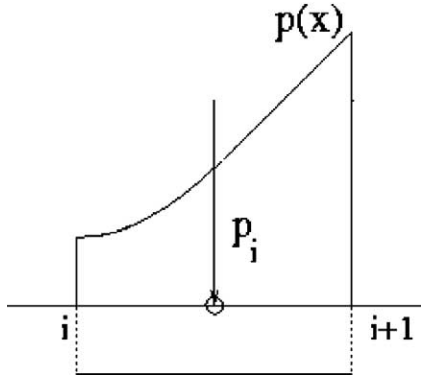

Fig. 4. Pressure distribution on a cell face.

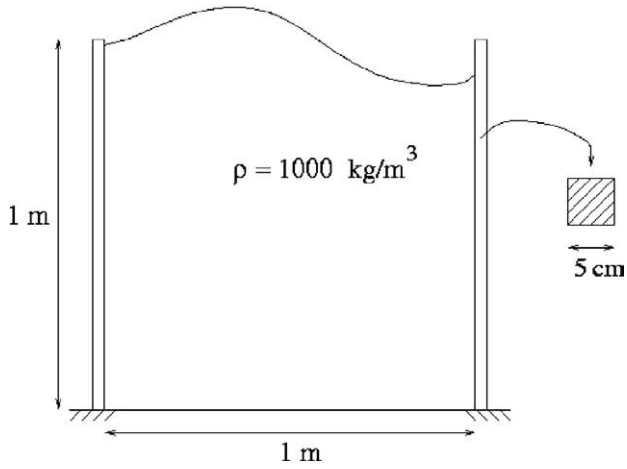

Fig. 5. Scheme of the domain with elastic walls.

The data transfer from CSD to CFD is less difficult and is performed by a simple data interpolation on the deformations. This is due to a better regularity of the physical phenomenon of structural deformation with respect to the pressure fluctuations.

The time-stepping algorithm works as follows. First, the partition method that we have developed performs a fluid dynamics simulation and the pressures on the solid walls and displacements of the points of the free surface are evaluated. Then, data are transferred to the CSD solver and the structural simulation is performed, in order to evaluate the deformations of the tank. These values are transferred to the CFD solver to update the boundary conditions. Besides, it is now possible to draw the new shape of the CFD domain and to update the computational grid, performing a new time step and continuing the time marching procedure with a new CSD simulation (performed on the grid which has been updated on the basis of the previous deformations).

5. Results

The test cases presented herein assume that the undeformed tank is a square box ($L = H = 1$ m) (Fig. 5), that the gravity acceleration is equal to the earthly value and that the tank is filled by water

($\rho = 1000$ kg m^{-3}). The vertical walls are made up of steel ($E = 198 \times 10^9$ Pa, $\nu = 0.3$) and are characterized by a square section with size $s = 5$ cm. The horizontal wall is rigid and the frictional resistance opposing the motion is neglected. For the CFD solver, a grid with 101×101 nodes has been adopted, while for the CSD solver an unstructured grid of 552 nodes and 877 elements, generated by the commercial code ANSYS 5.7 is used. The time step is 10^{-3} (non-dimensional units).

5.1. Tank motionless

In the first case, we assume that the tank is motionless and the fluid motion is induced by a perturbation on the free surface. The fluid is initially at rest, while the free surface has the following initial shape:

$$\eta(x, 0) = 0.005 \cdot \cos\left(\frac{2\pi}{\lambda}x\right),$$

with $\lambda = L/2, L/4, L/6$. This test case has been chosen because many theoretical and numerical results are available in literature for the case of a rigid tank [20,21,8,22,23] so we are interested in the evaluation of the influence of deformable walls on the solution. In a rigid tank, the initial perturbation causes the points of the free surface to oscillate in a sinusoidal way with a frequency given by $f_t = \sqrt{g/2\pi\lambda}$ [20]. In the present case, for each of the three values of λ, a similar behavior is registered, but the values of frequencies (Table 1) are different from the theoretical ones being the difference between 4% and 7%. Figs. 6, 7 and 8 show respectively the transient history of the horizontal displacement of a grid point located on the left wall at $y = 1$ m, for $\lambda = L/2$, $L/4$ and $L/6$. The analysis of these signals reveals that

Table 1
Main oscillation frequency ($\mathbf{f_s}$), minimum and maximum displacement of the left vertical wall, oscillation frequency of the free surface ($\mathbf{f_f}$), error on the continuity equation as a function of λ

λ	$\mathbf{f_s}$	Min. displ.	Max. displ.	$\mathbf{f_f}$	Err.
$L/2$	0.5489	-1.3623×10^{-3}	-1.37491×10^{-3}	0.5446	2.07×10^{-10}
$L/4$	0.7324	-1.3756×10^{-3}	-1.36292×10^{-3}	0.7374	5.67×10^{-10}
$L/6$	0.8544	-1.3742×10^{-3}	-1.36385×10^{-3}	0.9074	8.71×10^{-10}

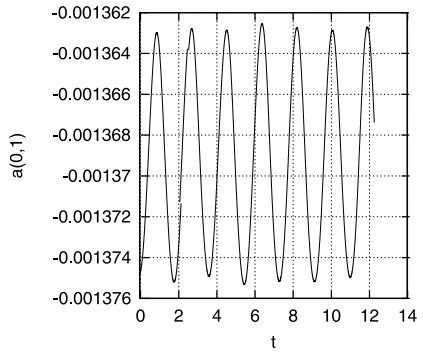

Fig. 6. Tank motionless: transient history of the horizontal displacement of the point located on the left wall at $y = 1$ m, for $\lambda = L/2$.

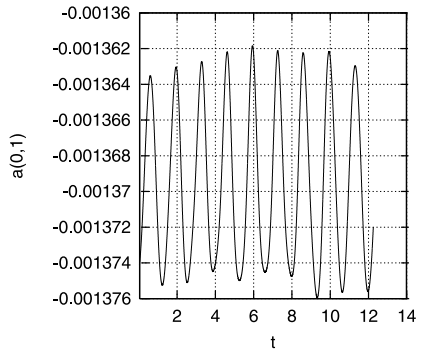

Fig. 7. Tank motionless: transient history of the horizontal displacement of the point located on the left wall at $y = 1$ m, for $\lambda = L/4$.

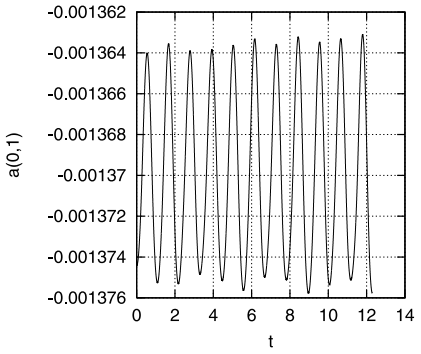

Fig. 8. Tank motionless: transient history of the horizontal displacement of the point located on the left wall at $y = 1$ m, for $\lambda = L/6$.

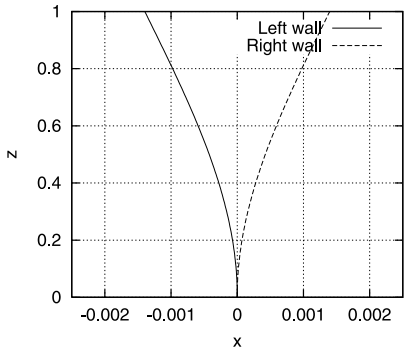

Fig. 9. Tank motionless: average deformed configuration of the vertical walls for $\lambda = L/2$.

also the vertical walls oscillate in a periodic way. For $\lambda = L/2$ only one frequency is observed, while for $\lambda = L/4$ and $L/6$ a second low frequency appears, whose value is a quarter of the main one.

Table 1 reports the values of the main frequency of oscillation of the grid point located on the left wall at $y = 1$ m ($\mathbf{f_s}$), with maximum and minimum value of the displacement (non-dimensional units). The fourth column indicates the value of the main frequency of oscillation ($\mathbf{f_f}$) of a point on the free surface ($\eta(0.25, t)$). Besides, for each case the maximum error on the continuity equation is evaluated by calculating the difference between the domain area at each time step and the original one ($L \cdot H$).

The values of the displacements of the vertical walls are compared to the ones obtained using the commercial code ANSYS 5.7, considering a cantilever beam subjected to a distributed pressure equal to the one produced by the liquid. The comparison shows a good agreement, because the difference is less than 1%. Fig. 9 shows the average deformed configuration of the vertical walls at $\lambda = L/2$. The scale of the horizontal displacements is quite different from the scale of the vertical extension of the walls, in order to better visualize the deformations. Fig. 10 shows the LIC (line integral convolution) representation at the time $t = 12.288$ for $\lambda = L/2$. It has been performed with the software visualization FLOVIS [24], and gives an idea of the particle trajectories during the oscillations.

5.2. Forced sway oscillations

In this case, we assume that the tank is forced to oscillate harmonically along the horizontal direction. A partially filled tank experiences violent fluid motion when subjected to periodic forces containing energy in the vicinity of the natural periods for the fluid motion inside the tank. The problem of small horizontal oscillations was extensively investigated in the past [21,8] for rigid containers. It has been shown that the response is the same as that of the undamped Duffing equation and changes from soft-spring (decreasing amplitude with increasing frequency) to hard-spring (increasing amplitude with increasing frequency) behavior as the ratio depth—width passes through a certain value. It is of course interesting to analyze the behavior of the system when the walls of the tank are no more rigid, in order to understand the influence of wall elasticity on the phenomenon. Unfortunately, experimental and numerical results related to this case are not available in literature for comparison. Thus, our results have to be considered as preliminary ones and the error that affects them has to be better quantified. The amplitude of the excitation is set equal to 0.005 non-dimensional units, while the circular frequency

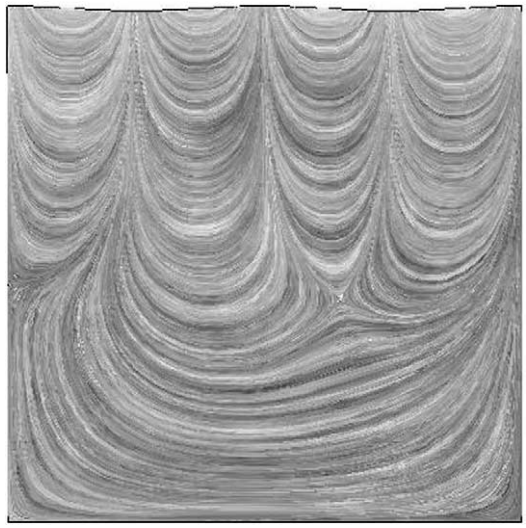

Fig. 10. Tank motionless: LIC representation for $\lambda = L/2$ at $t = 12.288$.

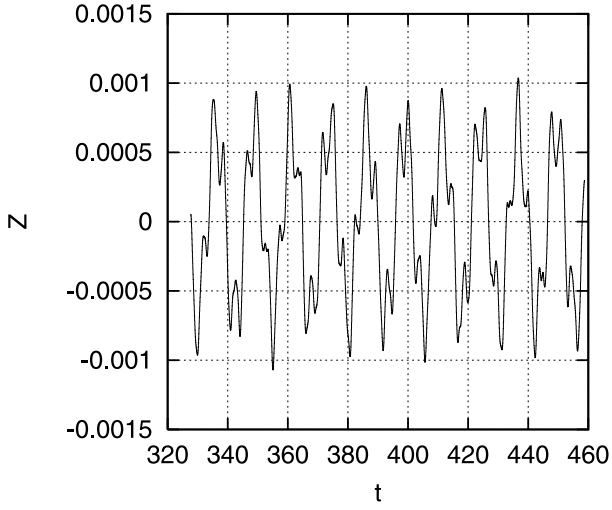

Fig. 11. Forced sway oscillations: wave elevation $\eta(0.025, t)$ as a function of time at $\omega = 0.5$.

of the external oscillation ω is varied between 0.1 and 0.6 non-dimensional units. For each simulation, a periodic oscillation of the vertical walls and of the free surface was found. Fig. 11 shows the free surface elevation as a function of time for $\omega = 0.5$. The maximum free surface elevation is evaluated and compared to the same values obtained in a rigid container [6]. These results are reported in Table 2. The comparison shows that in both cases the maximum value of η is growing with ω and the curve interpolating the available points clearly traces to the upper stable branch of an hard-spring amplitude response. However, even if the values are not really different, the tank with elastic walls seems to produce waves with larger amplitudes.

Table 2
Maximum free surface elevation in the present case and in the case of rigid tank as a function of ω

ω	Max η	Max η (rigid walls)
0.1	2.8320×10^{-5}	2.6912×10^{-5}
0.2	1.6912×10^{-4}	1.6830×10^{-4}
0.3	3.7890×10^{-4}	3.4513×10^{-4}
0.4	7.4913×10^{-4}	7.0477×10^{-4}
0.5	1.3812×10^{-3}	1.0700×10^{-3}
0.6	1.6613×10^{-3}	1.4904×10^{-3}

6. Conclusions

A numerical code for the study of the motion of an incompressible inviscid flow in a deformable tank has been presented. It is based on a method belonging to the partition treatment class, as the fluid and structural fields are solved by means of two distinct models. The fluid field is calculated by numerically solving the Laplace equation by a finite volume technique on a computational grid updated at each time step. The tank has been modelized by means of an unsteady finite element formulation using triangular elements and linear shape functions. The partition methods feature the advantage that also two commercial codes can be coupled, but are probably less accurate with respect to the methods of the *simultaneous treatment* class. Numerical results have been presented considering two cases: a tank motionless where the top surface is free and oscillates under the effects of perturbations; a tank forced to oscillate along the horizontal direction. In the last case, the external excitation frequency is varied in a range placed below the first natural frequency. The tank with elastic walls seems to produce waves with larger amplitudes with respect to the tank with rigid walls. The numerical code revealed to be very effective as it is very fast and guarantees the respect of the mass conservation. However the problems under investigation are very complex and require a deeper analysis, that will be the topics of future research.

References

[1] J. Mackerle, Fluid-structure interaction problems, finite elements and boundary elements approaches. A bibliography (1995–1998), Finite Elements Anal. Design 31 (1999) 231–240.
[2] F. Casadei, J.P. Halleux, A. Sala, F. Chille, Transient fluid-structure interaction algorithms for large industrial applications, Comput. Methods Appl. Mech. Engrg. 190 (2001) 3081–3110.
[3] O. Zienkiewicz, R.L. Taylor, The Finite Element Method, vol. 2, fourth ed., McGraw-Hill Book Company, New York, 1991.
[4] M. Gluck, M. Breuer, F. Durst, A. Halfmann, E. Rank, Computation of fluid-structure interaction on leghtweight structures, J. Wind Engrg. Indust. Aerodyn. 89 (2001) 1351–1368.
[5] Q. Zhang, T. Hisada, Numerical methods for FSI problems with strong dependence between fluid and structure, Comput. Methods Appl. Mech. Engrg. 190 (48) (2001) 6341–6357.
[6] E. Bucchignani, A numerical study of non-linear dynamics in a tank for aerospace applications, Appl. Numer. Math. 49 (3–4) (2004) 307–318.
[7] W. Tsai, D. Yue, Computations of nonlinear free-surface flows, Annual Rev. Fluid Mech. 28 (1996) 249–278.
[8] O. Faltinsen, A. Timokha, An adaptive multimodal approach to nonlinear sloshing in a rectangular tank, J. Fluid Mech. 432 (2001) 167–200.

[9] F. Stella, E. Bucchignani, True transient vorticity–velocity method using preconditioned Bi-CGSTAB, Numer. Heat Transfer Part B 30 (1996) 315–339.
[10] C. Hirsch, Numerical Computation of Internal and External Flows, vol. 1, Wiley, New York, 1991.
[11] J. Cranck, P. Nicholson, A practical method for numerical evaluation of solutions of partial differential equations of the heat conduction type, Proc. Cambridge Philos. Soc. 43 (50) (1947) 50–67.
[12] P.F. Galpin, G.D. Raithby, Treatment of non-linearities in the numerical solution of the incompressible Navier–Stokes equations, Internat. J. Numer. Methods Fluids 6 (7) (1986) 409–426.
[13] A. El-Zeiny, Nonlinear Time-Dependent Seismic Response of Unanchored Liquid Storage Tanks, Ph.D. Thesis, University of California, Irvine, CA, 2000.
[14] G. Guj, F. Stella, Numerical solutions of high-*Re* recirculating flows in vorticity-velocity form, Internat. J. Numer. Methods Fluids 8 (1988) 405–416.
[15] H. van der Vorst, Bi-CGSTAB, a fast and smoothly converging variant of Bi-CG for the solution of nonsymmetric linear systems, SIAM J. Sci. Statist. Comput. 13 (2) (1992) 631–644.
[16] A. Peters, Non-symmetric CG-like schemes and the finite element solution of the advection–dispersion equation, Internat. J. Numer. Methods Fluids 17 (1993) 955–974.
[17] O. Zienkiewicz, R.L. Taylor, The Finite Element Method, vol. 1, McGraw-Hill Book Company, New York, 1977.
[18] C. Farhat, M. Lesoinne, P. LeTallec, Load and motion transfer algorithms for fluid/structure interaction problems with non-matching discrete interface: momentum and energy conservation, optimal discretization and application to aeroelasticity, Comput. Methods Appl. Mech. Engrg. 157 (1998) 95–114.
[19] F.P. Preparata, Planar point location revisited, Internat. J. Found. Comput. 1 (1990) 71–86.
[20] O. Faltinsen, A nonlinear theory of sloshing in rectangular tanks, J. Ship Res. 18 (4) (1974) 224–241.
[21] O. Faltinsen, O. Rognebakke, I. Lukowsky, A. Timokha, Multidimensional modal analysis of nonlinear sloshing in a rectangular tank with finite water depth, J. Fluid Mech. 407 (2000) 201–234.
[22] A. Bermudez, R. Rodriguez, Finite element computation of vibration modes of a fluid-system, Comput. Methods Appl. Mech. Engrg. 119 (1994) 335–370.
[23] A. Bermudez, R. Rodriguez, Finite element analysis of sloshing and hydroelastic vibrations under gravity, Math. Modelling Numer. Anal. 33 (1999) 305–327.
[24] B. Sikorski, P. Leoncini, FLOVIS: yet another numerical–experimental visualisation system, in: 8th Int. Symposium on Flow Visualization, Sorrento, Italy, 1998.